

Properties of Large Core Polymer Optical Bend Waveguides

Václav PRAJZLER, Marian KNIETEL, Petr JASEK

Dept. of Microelectronics, Faculty of Electrical Engineering, Czech Technical University,
Technická 2, 166 27 Prague, Czech Republic

Vaclav.Prajzler@fel.cvut.cz

Submitted October 9, 2018 / Accepted December 5, 2018

Abstract. We report about properties of large core plastic planar optical bend waveguides. The dimensions of the waveguides were to be compatible with the commonly used plastic optical fiber with diameter $750\ \mu\text{m}$ and the bend radii of the waveguides varied from 30 to 1 mm. The waveguides were made by engraving of a U-groove by using CNC machining into poly(methyl methacrylate) substrate; the waveguide core layers were made of Norland Optical Adhesive UV photopolymer. We experimentally confirmed that fabricated bends may have the total bend losses A for radii 30 mm 4.1 dB/cm at 850 nm, 4.8 dB/cm at 650 nm and 5.63 dB/cm at 532 nm. These bend waveguides are viable for short reach visible and infrared optical communication with easy and low cost installations.

Keywords

Optical bend waveguides, multimode waveguides, polymer

1. Introduction

Nowadays, data transitions, which have been realized via electrical metallic wires, are gradually substituted by optical multimode waveguides connections for Short Reach (SR, up to 300 m), Extra Short Reach (ESR, up to 5 cm) and also Ultra Short Reach distance (USR, up to even 1 cm). The main advantage of the optical connections is that they are not susceptible to any radio-frequency interference or any cross-talks influences [1].

Last but not least, a significant advantage of the optical connections is a possibility of using polymer materials for many of the construction elements in the optical waveguide circuits or photonics structures including bend waveguides, what means simple, environmentally friendly as well as low cost technological solutions [2].

Optical bend waveguides are essential parts of basic blocks of integrated optics and photonics devices, whose importance sustainably grows with an increasing degree of integration in the frame of high-density photonics circuits.

Such basic building blocks have been developed for a couple of years and are also well characterized which concerns their utilization in the single-mode regime [3–5]. In the literature several types of optical bend waveguides have been already presented:

- bend waveguides described by D. Israel [6] and S. Musa [7]; this will be in more details mentioned later,
- single-mode polymer SU-8 2000 waveguide [8], with thickness around $1.7\ \mu\text{m}$ and having different core widths (1.2, 1.6, 2.0, 2.4 and $2.8\ \mu\text{m}$) and bending radius (300, 200, 150, 100, 75, 50 and $25\ \mu\text{m}$),
- multimode bend optical waveguides based on silicon rib structures (height of $28\ \mu\text{m}$ and width $25\ \mu\text{m}$); these S-bend structures have the radius ranging from 2 to 20 mm and the bend offset $0.5\ \text{mm}$ [9],
- fully embedded and air-exposed curved waveguides with a $50\ \mu\text{m} \times 50\ \mu\text{m}$ cross section having 10 mm bending radius limit [10],
- 90° bend and S-bend siloxane OE-4140 (core) and OE-414 (cladding) multimode waveguides having typical dimensions $50\ \mu\text{m} \times 50\ \mu\text{m}$ [11],
- multimode bend waveguides with dimensions $50\ \mu\text{m} \times 50\ \mu\text{m}$, $75\ \mu\text{m} \times 50\ \mu\text{m}$ and $100\ \mu\text{m} \times 50\ \mu\text{m}$ (wide \times high) made of acrylate polymer TruemodeTM from Exxelis Limited deposited on FR4 wafer intended for wavelength of 850 nm and the refractive index of the core was $n_{\text{core}} = 1.5560$ and that of the cladding was $n_{\text{clad}} = 1.5264$ [12],
- polymer multimode waveguide splitter having input waveguide core width $100\ \mu\text{m}$ and ended by S-bend waveguide with different core widths (20, 40, 60 and $80\ \mu\text{m}$); detailed study was presented in [13].

Up to now only one paper has dealt with planar multimode bends having large core waveguide [14]. The authors presented the properties of the bend waveguides with dimensions $600\ \mu\text{m} \times 600\ \mu\text{m}$ having bending radii 15, 20, 30 or 40 mm. The cores of them were made of SU8 2005 photoresist epoxy resin polymer and the claddings were made of poly(methyl methacrylate) PMMA. The authors

measured the properties of the bends at three wavelengths (850, 1310, and 1550 nm) and their lowest bending loss for the 15 mm bending radius was 6 dB/cm.

Papers on large core optical splitters [15–17] and wavelength division multiplexing module with thin film filters [18] prove that it is in principle possible to make multimode optical planar waveguides structures using large core waveguides that would have a good application potential. The main advantage of them, i.e. large core size that ease their installation, together with a low cost, has been already capitalized in automobile networks. There, they enable using simple plug connectors, which do not require sophisticated knowledge or any special equipment and technically skilled workers, in spite of the case of using single-mode optical waveguides or standard multimode waveguides having the core width 50 μm or 62.5 μm .

However, there is still a gap in our knowledge on such solution, and it concerns a combination of large core waveguides and extend of their curvature (bending) and how it may influence their waveguiding properties, especially what concerns their total bend losses.

In this paper we are going to focus on large core planar bend waveguides, whose dimensions are optimized for large core Plastic Optical Fiber (POF) type SH 3001 (MITSUBISHI RAYON CO., LTD ESKA OPTICAL FIBER DIVISION). The core layer of the fiber is made from polymethyl-methacrylate resin with diameter of the core 735 μm and refractive index $n_f = 1.49$ ($\lambda = 650$ nm) and cladding layer is made from fluorinated polymer with cladding diameter 750 μm , and numerical aperture (NA) is 0.5. We have already shown that Norland Optical Adhesives (NOA) UV glues had suitable properties for using as the waveguide core materials as it had low optical losses in the spectral region from visible to infrared [19] and was why our bends have the core waveguides made from UV photopolymer NOA and the substrate and cover layers are made from PMMA. Bending radius is from 1 to 30 mm.

The design of the bend waveguides was done exactly for assembling to the POFs (plastic optical fibers), i.e., to operate at the wavelength of 650 nm (red light). We found it interesting to supplement also the calculation and simulation for 532 and 850 nm (even though, at the moment, optical communication via POF waveguides do not even consider other but using that 650 nm).

2. Modeling of Multimode Bend Waveguides

The cross section of the multimode rectangular waveguides used for the bend is shown in Fig. 1(a) and cross section of the pertinent bend waveguide is shown in Fig. 1(b). The core waveguiding layer is made from UV NOA photopolymer with refractive index n_f and this layer is completely surrounded by cladding formed by PMMA polymer with refractive index n_c . Because the substrate and

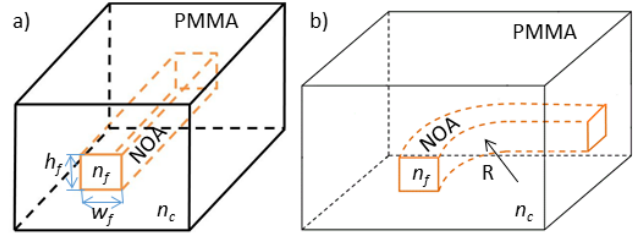


Fig. 1. (a) Cross-sectional view of the rectangular optical waveguide used for bends (substrate and cover layers is made from the same material), (b) geometrical structure of the proposed bend waveguide.

cover layer are made from the same material and, of course, have the same refractive indices, this will be a symmetrical optical waveguide. The design of the bend waveguide was made for the following radii R : 30, 20, 10, 6, 5, 4, 3, 2 and 1 mm. The width w_f and the height h_f of the waveguides were the same (750 μm) and the structure was designed for three wavelengths: 532, 650 and 850 nm.

Before practical realization of the bend waveguides we calculated their properties by the analysis published by D. Israel [6] and S. Musa [7]. The authors derived analytically the expression for transmission T of the 2D uniform distribution through the bend as a function of radii R (1):

$$T = \frac{P_{\text{out}}}{P_{\text{in}}} = 1 - \frac{1}{2}K - \frac{1}{6}K^2 - \frac{1}{8}K^3 - \frac{1}{8}K^4 \quad (1)$$

where P_{in} is the input optical power, P_{out} is the output optical power from the bend waveguide and K is the constant defined by the relationship (2):

$$K = \frac{w_f}{NA^2 \cdot R} \quad (2)$$

where w_f is the width of the waveguide core, R is the radius of the bend curvature and NA is the numerical aperture given by (3):

$$NA = \sqrt{n_f^2 - n_c^2} \quad (3)$$

where n_f and n_c are the refractive indices of the waveguide core layer and cladding layer, respectively. The relation (1) shows the agreement with the results of two-dimensional and three-dimensional ray-tracing modeling performed on bent waveguides with different bend radii [7], but equation (1) is valid only when $K < 0.5$ [6].

Transmission optical losses TL of the bend waveguide are then given by (4):

$$TL = -10 \cdot \log(T). \quad (4)$$

Total losses T_{LOS} of the bend waveguide are given by (5) [14]:

$$T_{\text{LOS}} = L_c + PR_L + TR_L + RD_L. \quad (5)$$

The sum of the input and output coupling losses L_c can be calculated by (6) [14]:

$$L_c = R_L + A_L + NA_L + L_{\text{sc}} \quad (6)$$

where R_L means Fresnel reflection losses on two interfaces and it can be expressed by (7):

$$R_L = 20 \cdot \log_{10} \frac{4n_1 n_f}{(n_1 + n_f)^2} \quad (7)$$

where n_1 is refractive index of the fiber core layer (in our case $n_1 = 1.49$) and n_f is the refractive index of the bend core waveguide.

The cross-section mismatch loss A_L , caused by a coupling of a circular fiber to a rectangular waveguide between the input fiber and the bend waveguide, is given by the following equation (8):

$$A_L = 10 \cdot \log_{10} \frac{\pi c^2}{w_f h_f} \quad (8)$$

where c is the radius of the POF core (in our case $369 \mu\text{m}$) and w_f and h_f are the width and height of the bend waveguide (in our case $w_f = h_f$, and it is $750 \mu\text{m}$). Numerical aperture mismatch loss NA_L is the loss given by the difference in the NA values arising between the optical waveguide and the fiber at the receiver side and can be calculated as follows (9) [14, 20]:

$$NA_L = 10 \cdot \log_{10} \left(\frac{NA_1}{NA_2} \right)^2 \quad (9)$$

where NA_1 and NA_2 mean the values of numerical apertures of the bend and the output POF waveguides (in our case POF $NA 0.5$, NA values are given in Tab. 1), respectively.

L_{sc} is the scattering loss resulting from the roughness of the waveguide end faces, which leads to scattering into a wide range of angles. This loss is minimized at the transmitter side if a well-cleaved fiber is butt coupled inside the waveguide channel and it is more significant at the receiver side where the light is coupled from the waveguide end into the detector [14].

PR_L is dominated by scattering of energy due to waveguide sidewall roughness. This can be measured by using the cut-back method.

TR_L are the transition losses arising from transition between straight and bend waveguide occurring at the junction (interface) between two waveguide structures (straight and bent), which result in mismatch in the modes. Several guided rays in the first waveguide section can exceed the critical angle in the second waveguide section and then can escape outward. According to [14], in the large core cross-section waveguides, which is our case, the number of the modes is very high, so the transition losses are expected to be bigger than the radiation losses.

RD_L are the radiation losses resulting from the radiated energy in the bend part of the waveguide (see also [20]).

For the precise design and calculation of properties of the bend waveguide we measured the values of the refractive indices by dark-mode spectroscopy at five wavelengths

λ (nm)	532	650	850	
n_c (PMMA) (-) [23]	1.495	1.489	1.486	
n_f (NOA) (-) [23]	1.564	1.555	1.550	
NA (-)	0.459	0.450	0.440	
R_L (dB)	0.005	0.004	0.003	
NA_L (dB)	0.743	0.954	1.091	
K	$R = 30\text{mm}$	0.118	0.124	0.129
	$R = 20\text{mm}$	0.178	0.187	0.193
	$R = 10\text{mm}$	0.355	0.373	0.386
	$R = 8\text{mm}$	0.444	0.467	0.482
	$R = 7\text{mm}$	0.508	0.533	0.551

Tab. 1. Values of refractive indices and calculated numerical aperture and K constant (equation (2)) ($w_f = 750 \mu\text{m}$, λ - wavelength, n_c - refractive index of PMMA substrate and cladding, n_f - refractive index of NOA core layer).

(473, 632.8, 964, 1311 and 1552 nm) [21] [22]. The values of the refractive indices for three wavelengths (532, 650 and 850 nm) used for the modeling of the properties of optical planar bends were calculated from this measurement by Cauchy dispersion fitting (see Tab. 1). These values of the refractive indices have been already published in [23].

Table 1 also shows the calculated values of numerical aperture NA , Fresnel reflection losses R_L , Numerical aperture mismatch loss NA_L and constant K . The design was done for the large core waveguide having $w_f = 750 \mu\text{m}$, for three wavelengths (532, 650 and 850 nm) and five bend radii ($R = 30, 20, 10, 8$ and 7 mm).

As mentioned above, equation (1) is valid only for $K < 0.5$, so for our case (see Tab. 1) it is possible to determine the transmission loss TL only up to $R \geq 8$ mm. Calculated transmission optical losses TL (equation (4)) depending on bend radius are shown in Fig. 2. The figure clearly shows that the optical transmission losses TL are decreasing with the increasing bend radius. It also shows that the longer wavelengths make the effect of the bending slightly more significant.

The design of the bend waveguides was refined by computer modeling done using Beam Propagation Method (BPM), which used the BeamPROP software provided by RSoft. The result of the simulation was the 2D layout bend waveguide in which a dependence of the normalized output optical power on the radius of the bending of the waveguide was further simulated. The modeling was done by 2D channel with multimode source and the total power was calculated by the used simulation.

Example of the layout done by the simulation is given in Fig. 3(a), where the contour of the refractive index profile of the $750 \mu\text{m}$ wide bend waveguide with radius 30 mm having waveguiding NOA layer ($n_f = 1.555$) and PMMA ($n_s = 1.489$) cladding layer, given for the wavelength 650 nm, is shown. The results of the simulation for

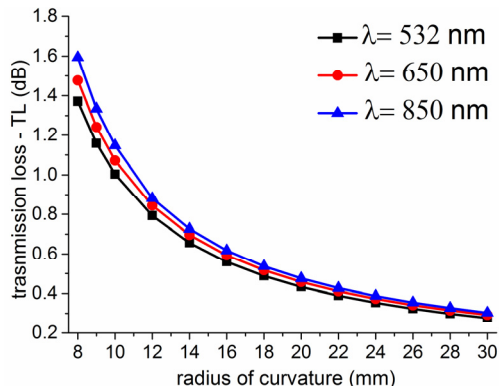


Fig. 2. Design of the transmission optical losses TL for the bend waveguide using NOA (core)/PMMA (cladding).

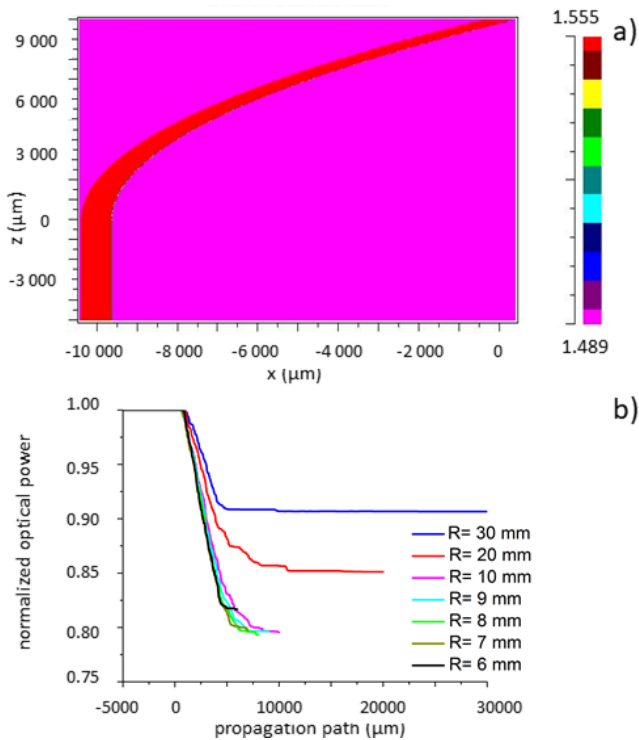


Fig. 3. The results of the simulation of the bend waveguide done by the BeamPROP software (a) refractive index profile of the PMMA/NOA bend waveguide (width $750 \mu\text{m}$, $n_i = 1.555$, $n_c = 1.489$, $\lambda = 650 \text{ nm}$, radius $R = 30 \text{ mm}$), (b) the results of the simulation of the bend for radius $R = 30, 20, 10, 9, 8, 7$ and 6 mm .

various radii of the bends are given in Fig. 3(b) ($R = 30, 20, 10, 9, 8, 7$ and 6 mm).

From Fig. 3(b) it follows that for the radii $R = 10, 20$ and 30 mm the higher radius the higher the optical power; for smaller R ($R < 9 \text{ mm}$) the optical power almost does not change. It might be so because in the multimode waveguides a strong interaction occurs between the guided modes which prevents the modes to get stabilized; another reason might be that due to the low radius a part of the optical energy is emitted into the cladding. This explanation is supported by the calculation done according to Israel [6] for the constant K , as given in Tab. 1. However, it can be done only if $K < 0.5$ and it means that equation (1) in the case that $R \leq 7 \text{ mm}$ cannot be used.

3. Experiments

For fabrication of the large core bend waveguides with radius $10, 20$ and 30 mm (sample #1) we used a similar fabrication process, which has been already presented for large core $1 \times 2Y$ splitter assembled with 1 mm POF waveguides [24] or $910 \mu\text{m}$ core optical fibers (FG910LEC Thorlabs Inc.) [19]. Here we made U-grooves with dimensions $750 \mu\text{m} \times 750 \mu\text{m}$ (wide \times high) needed for filling with the waveguide material into the 3 mm thick PMMA substrate. This procedure was again done by the CNC (Computer Numerical Control) NONCO Kx3 milling machine. The milling tool had 0.6 mm wide spindle, rotation speed was 1800 rpm/min and moving speed was 36 mm/min . Then, into every inputs and outputs of the made U-grooves we inserted 15 cm long pigtail plastic optical fibers (ESKATM Premier Polyethylene-jacketed Optical Fiber Cord SH-3001 manufactured by Mitsubishi Rayon Co., Ltd.), whose faces were polished before being inserted. Next the U-groove space, between the input and output fiber waveguides, was filled with optically clear UV photopolymer NOA73 (Norland Products Inc.) that was then hardened by UV curing. Finally, the made bend waveguides were covered by PMMA sheet.

The bend waveguides having smaller radii ($R = 1$ to 6 mm) were realized as follows: both ends of the U-grooves made by the CNC machine (as above) were, before filling with NOA polymer, perpendicularly fixed with polymer foils covered by the SP-3 (ELCHEMCo) separator. Such arrangement was needed to prevent spilling the NOA polymer out of the made U-grooves and made feasible removing of the foils from the grooves after the hardening. The results were smooth optical facets without a need to polish them for optical measurement. This way we made the samples of the bend waveguides, each of them contained three bend waveguides, one of them having the bend radii $1, 3$ and 5 mm (sample #3) and the other one had the radii $2, 4$ and 6 mm (sample #2).

4. Results

Figure 4 shows the photos of the made bend waveguides. Figure 4(a) gives a top view of the bend waveguides

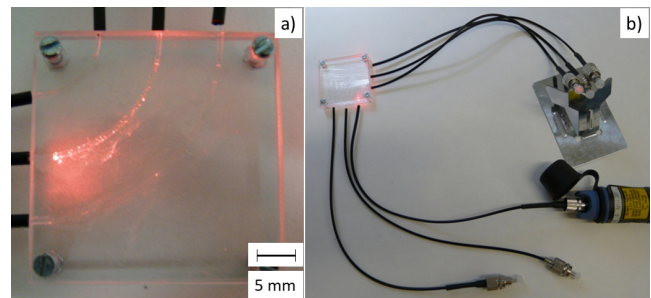


Fig. 4. (a) Images of PMMA substrate with U-grooves for bend waveguides with radius $R = 30, 20$ and 10 mm , (b) images of the bend waveguide transmitting optical light at 635 nm .

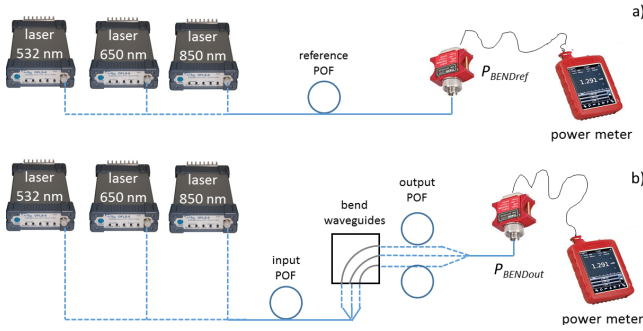


Fig. 5. Setup for the total bend losses α measurements: (a) measurement of the reference optical power $P_{BENDref}$, (b) measurement of the optical power $P_{BENDout}$.

with bigger radii ($R = 30, 20$ and 10 mm) and middle waveguide connected to red light and Figure 4(b) shows the final bend waveguides ($R = 30, 20$ and 10 mm) with assembling inputs/outputs fiber and one channel connected to a laser tester FLS operating at wavelength 635 nm. Here the guiding of the red light is seen, which is transmitted through the bend waveguide (with $R = 10$ mm) to the output fiber waveguide.

The total bend losses α were measured by a setup shown in Fig. 5 and then they were calculated from (10). The bend losses A modified with regard to the lengths of the bend waveguides were then calculated from (11):

$$\alpha = -10 \cdot \log \frac{P_{BENDout}}{P_{BENDref}} \text{ [dB]}, \quad (10)$$

$$A = \frac{\alpha}{L} \text{ [dB/cm]}. \quad (11)$$

The total bend losses α and the bend losses A are the measured values of the optical losses, which are generally considered to be the sum of the total losses T_{LOS} calculated from (5), where $P_{BENDref}$ is the output optical power coming from the laser source and passing through the reference POF fiber (see Fig. 5a), $P_{BENDout}$ is the optical power measured separately for different output bend waveguides (see Fig. 5b) and L is the length of the bend waveguides. The total bend losses α and the bend losses A modified regarding to the lengths of the bend waveguides were measured at three wavelengths: 532 nm using Nd:YVO₄ laser, 650 nm using OFLS-5 FP-650 laser and 850 nm using OFLS-6 LD-850 laser. Optical power was measured by power meter Thorlabs PM200 with silicon S151C probe.

The measurement of the total bend losses α for the bend waveguides with larger radii ($30, 20$ and 10 mm) started by measurement of reference optical power $P_{BENDref}$ using 30 cm long patch cord of optical $750 \mu\text{m}$ POF fiber. After that we measured optical power $P_{BENDout}$ for each bend waveguide using connection to input/output fibers.

The reference optical power $P_{BENDref}$ for the total bend losses α of bends with smaller radii ($1-6$ mm) was measured by the same way as in the previous case; however, because small dimensions of these bend waveguides did not allow for using any solid connecting, they were meas-

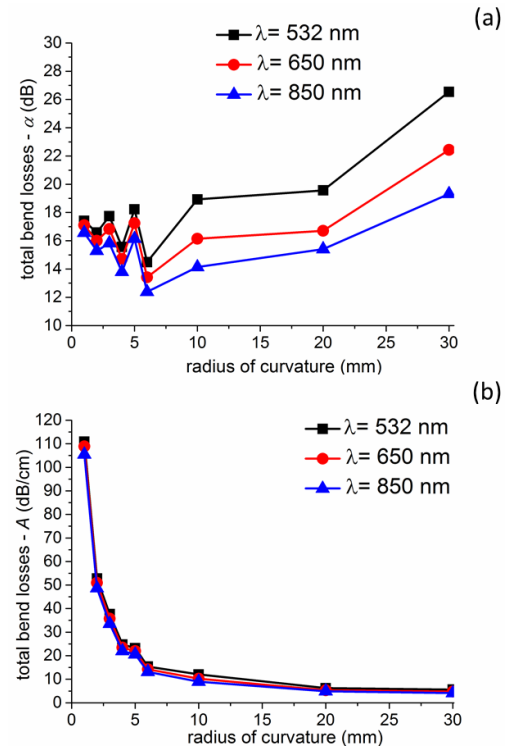


Fig. 6. Bend losses measured at $532, 650$ and 850 nm: (a) the total bend losses α , (b) the bend losses A modified with regard to the lengths of the bend waveguides.

ured directly on the optical bench with help of pigtailed with POF fibers, that were drawn as near as possible to the samples (instead of sticking to them). The light into the bend waveguides were coupled from the laser into the bend channel using the 15 cm long $750 \mu\text{m}$ wide core plastic fiber which was precisely aligned using high-precision 3-axis stages. The output light power intensity was then collected by similar POF fiber as the input fiber (as above: 15 cm long and $750 \mu\text{m}$ wide-core) and detected again by the silicon detector and Thorlabs power meter.

The results gained by the measurement of the bend waveguides are shown in Fig. 6 where Figure 6(a) shows the relations of the total bend losses α on the radius R and Figure 6(b) shows the bend losses A that were modified regarding to the lengths of the bend waveguides.

In Fig. 6a it seems that for $R = 1$ to 6 mm the values of the total bend losses α oscillate around a mean value, and it hints that a certain deterioration of the waveguiding effect probably occurred there, which might be caused by a fact that the optical contact was not equally efficient for each waveguide and a substantial part of the optical energy might be emitted into the cladding. What concerns the higher radius ($R > 10$ mm), the losses α are the highest ones probably as a consequence of the longer of lengths of the waveguides.

For bend waveguides with small radii ($R < 6$ mm), whose straight part is rather short, the TR_L transition losses are marginal and the same is true for the propagation losses PR_L . Substantial part of the losses in such strongly bend waveguides is radiation losses RD_L , which results from the

energy radiated into the cladding in the bent part of the waveguides.

Bigger radii of the bends ($R > 10$ mm) make the radiation losses RD_L lower comparing with those of the less bent waveguides, and dominant part of the losses will be here propagation losses PR_L . This is illustrated in Fig. 6(b), which shows the results of the measurement of the bend losses A , which were modified according to the lengths of the waveguides. Here the relations between the losses A and the pertinent radii are clearly shown, i.e. the smaller is the radius the higher the losses are. When the radii become bigger (above 20 mm) then the losses A get decrease very slowly as the dominant effect is not its radius any more. Additional effect is the wavelength: at shorter wavelengths the losses are higher and vice versa. For higher R the effect of the wavelength is smaller, i.e., if $R = 20$ or 30 mm, then A is very similar for all the used wavelengths (i.e., 532, 650 and 850 nm).

Assuming for simplification that the measured values of the total bend losses α (equation (10)) are equal to the total losses T_{LOS} (given by (5)) we can determine the sum of remaining losses P_{LOS} , which will consist of PR_L (propagation losses) + TR_L (transition losses) + RD_L (radiation losses); such losses cannot be measured independently. To determine P_{LOS} we calculated the Fresnel reflection losses R_L (equation (7)) (for the refraction indices used for calculation see Tab. 1), the values of the cross-section mismatch losses A_L are 1.189 dB (equation (8), where $w_f = h_f = 750$ μm , i.e., the dimensions of the channel bend waveguides, and $c = 369$ μm , which is the radius of the POF fiber) and calculated values of the Numerical aperture mismatch loss NA_L (equation (9)), which are shown in Tab. 1. Summarizing $R_L + A_L + NA_L$ we get 1.94 dB for the wavelength 532 nm, 2.15 dB for 650 nm and 2.28 dB for 850 nm, respectively. Finally, we get the values of the remaining losses P_{LOS} , which were determined by abstraction of calculated losses (sum of L_{sc} , i.e., the scattering

losses resulting from the roughness of the waveguide end faces, PR_L , i.e., the propagation losses, TR_L , i.e., the transition losses arising from the transition between straight and bend and RD_L , i.e., the radiation losses) from the experimentally measured total bend losses α . The resultant P_{LOS} are given in Tab. 2.

Such losses decrease with longer wavelengths, the highest value 21.07 dB was found at the shortest used wavelength (532 nm) and $R = 30$ mm. In spite of it, the lowest optical loss 7.59 dB was found at 850 nm when $R = 10$ mm. At the smaller radii $R < 9$ mm the results might be strongly affected by emission of the radiation towards the cladding. As we have already mentioned, the total losses of the waveguides having small radii are far more sensitive towards the way how the light is coupled into the waveguide.

5. Conclusion

We have experimentally studied properties of the large core polymer optical bend waveguides 750 μm wide and 750 μm high with the bend radii from 30 mm to 1 mm. The study was done for possible applications in POFs assembled structures, which up to now has operated exclusively at 650 nm, however, we found interesting to utilize the possibility offered by the used experimental method and include also the consideration concerning another two wavelengths, 532 and 850 nm.

We started with modeling of thought properties by the analysis published by D. Israel [6] and S. Musa [7] and then we used beam propagation method to calculate them. The bend waveguide structures were made by CNC engraving into PMMA substrate and NOA core waveguide photopolymer was then hardened by the UV radiation. Finally, PMMA polymer was used as cover cladding.

The measurement of the total bend losses showed that the lowest losses (12.4 dB) was found with the waveguide with bend radius of 6 mm. Higher values of the losses of the waveguides with smaller radii were probably caused by emission of the optical radiation into the cladding layer (radiation losses RD_L result from the radiated energy in the bent part of the waveguide). The bend waveguides with bigger radii ($R > 6$ mm) are more affected by the lengths of the guides,; which means that the part of the propagation losses PR_L in the whole sum of the losses is bigger.

The measurement of the total bend losses A , which are modified with regard to the lengths of the bend waveguides, proved that for the radii $R = 1$ to 6 mm the losses for the whole bend are higher than those for larger radii $R = 10, 20, 30$ mm and increased above 13 dB/cm. The lowest total bend losses A for $R = 30$ mm are 5.63 dB/cm at 532 nm, 4.76 dB/cm at 650 nm and 4.1 dB/cm at 850 nm. Such trend of the relations is in a good agreement with the simulation done by means of BPM method and by calculation concerning the samples with higher values of R ($R = 10, 20$ and 30 mm).

sample	bend radius R (mm)	λ (nm)		
		532	650	850
		remaining losses P_{LOS} (dB)		
#1	30	21.07	16.47	14.20
	20	13.95	10.67	8.84
	10	11.66	10.01	7.59
#2	6	12.55	11.27	10.10
	4	13.62	12.56	11.52
	2	14.64	13.85	13.01
#3	5	16.29	15.09	13.86
	3	15.80	14.68	13.55
	1	15.47	14.95	14.28

Tab. 2. Sum of remaining losses P_{LOS} (sum of L_{sc} the scattering loss resulting from the roughness of the waveguide end faces, PR_L the propagation losses, TR_L the transition losses arising from the transition between straight and bend, RD_L the radiation losses) for different bend radius.

The most similar large core bend waveguides, though smaller ($600\ \mu\text{m} \times 600\ \mu\text{m}$) than our ones and designed for IR region (850, 1310 and 1550 nm), were published in [14]. The lowest value of bending loss presented by those authors occurred at the shortest wavelength of the light source (850 nm) used by them and they found the bending loss for a 15 mm bending radius as high as 6 dB/cm, which is around 2 dB/cm higher than in our case. Furthermore, our bend waveguides have the bigger core (750 μm), and it means that it allows for using also in the visible range of the spectra, which makes it the main achievement of our approach.

Though the intention of the presented research was not any technological solution our results proved that large core bend waveguides could be fabricated by easy fabrication procedure and can be used as the low cost optical devices for distribution of the optical signal for very short distance connection (used for example in the automotive industry). The main advantages of our approach are simple fabrication process and due to large dimensions of the device also simple manipulation allowing for installations also by any less professional staffers.

Acknowledgments

Our research has been supported by the Czech Technical University in Prague with the SGS program (SGS17/188/OHK3/3T/13) and by the "Center of Advanced Applied Natural Sciences", Reg. No. CZ.02.1.01/0.0/0.0/16_019/0000778, which was supported by the Operational Program Research, Development and Education and co-financed by the European Structural and Investment Funds as well as by the state budget of the Czech Republic.

References

- [1] MILLER, D. A. B. Physical reasons for optical interconnection. *International Journal of Optoelectronics*, 1997, vol. 11, no. 3, p. 155–168.
- [2] MA, H., JEN, A. K. Y., DALTON, L. R. Polymer-based optical waveguides: Materials, processing, and devices. *Advanced Materials*, 2002, vol. 14, no. 19, p. 1339–1365. DOI: 10.1002/1521-4095(20021002)14:19<1339:AID-ADMA1339>3.0.CO;2-O
- [3] MARCATILI, E. A. Bends in optical dielectric guides. *Bell System Technical Journal*, 1969, vol. 48, no. 7, p. 2103–2132. DOI: 10.1002/j.1538-7305.1969.tb01167.x
- [4] CHERCHI, M., YLINEN, S., HARJANNE, M., et al. Dramatic size reduction of waveguide bends on a micron-scale silicon photonic platform. *Optics Express*, 2013, vol. 21, no. 15, p. 17814–17823. DOI: 10.1364/OE.21.017814
- [5] LI, G., YAO, J., LUO, Y., THACKER, H., et al. Ultralow-loss, high-density SOI optical waveguide routing for macrochip interconnects. *Optics Express*, 2012, vol. 20, no. 11, p. 12035–12039. DOI: 10.1364/OE.20.012035
- [6] ISRAEL, D., BAETS, R. Study of multimode polymeric waveguide bends for backplane optical interconnect. In *The 4th Microoptics Conference and The 11th Topical Meeting on Gradient-Index Optical Systems (MOC/GRIN93)*. Kawasaki (Japan), 1993, No. B4, p. 26–29.
- [7] MUSA, S., BORREMAN, A., KOK, A. A. M., et al. Experimental study of bent multimode optical waveguides. *Applied Optics*, 2004, vol. 43, no. 30, p. 5705–5707. DOI: 10.1364/AO.43.005705
- [8] YANG, B., YANG, L., HU, R., et al. Fabrication and characterization of small optical ridge waveguides based on SU-8 polymer. *Journal of Lightwave Technology*, 2009, vol. 27, no. 18, p. 4091–4096. DOI: 10.1109/JLT.2009.2022285
- [9] REZEM, M., GUNTHER, A., ROTH, B., et al. Low-cost fabrication of all-polymer components for integrated photonics. *Journal of Lightwave Technology*, 2017, vol. 35, no. 2, p. 299–308. DOI: 10.1109/JLT.2016.2639740
- [10] BAMIEDAKIS, N., PEMTY, R. V., WHITE, I. H. Compact multimode polymer waveguide bends for board-level optical interconnects. *Journal of Lightwave Technology*, 2013, vol. 31, no. 14, p. 2370–2375. DOI: 10.1109/JLT.2013.2265774
- [11] BAMIEDAKIS, N., BEALS, J., PENTY, R. V., et al. Cost-effective multimode polymer waveguides for high-speed on-board optical interconnects. *IEEE Journal of Quantum Electronics*, 2009, vol. 45, no. 4, p. 415–424. DOI: 10.1109/JQE.2009.2013111
- [12] PAPAKONSTANTINO, I., WANG, K., SELVIAH, D. R., et al. Transition, radiation and propagation loss in polymer multimode waveguide bends. *Optics Express*, 2007, vol. 15, no. 2, p. 669–679. DOI: 10.1364/OE.15.000669
- [13] HASHIM, A., BAMIEDAKIS, N., PEMTY, R. V., et al. Multimode polymer waveguide components for complex on-board optical topologies. *Journal of Lightwave Technology*, 2013, vol. 31, no. 24, p. 3962–3969. DOI: 10.1109/JLT.2013.2278382
- [14] HAMID, H. H., FICKENSCHER, T., THIEL, D. V. Experimental assessment of SU-8 optical waveguides buried in plastic substrate for optical interconnections. *Applied Optics*, 2015, vol. 54, no. 22, p. 6623–6631. DOI: 10.1364/AO.54.006623
- [15] EHSAN, A. A., SHAARI, S., ABD RAHMAN, M. K. Acrylic and metal based Y-branch plastic optical fiber splitter with optical NOA63 polymer waveguide taper region. *Optical Review*, 2011, vol. 18, no. 1, p. 80–85. DOI: 10.1007/s10043-011-0036-9
- [16] PRAJZLER, V., MAŠTERA, R., ŠPIRKOVÁ, J. Large core three branch polymer power splitters. *Radioengineering*, 2015, vol. 24, no. 4, p. 885–891. DOI: 10.13164/re.2015.0885
- [17] TAKEZAWA, Y., AKASAKA, S., OHARA, S., et al. Low excess losses in a Y-branching plastic optical waveguide formed through injection molding. *Applied Optics*, 1994, vol. 33, no. 12, p. 2307–2312. DOI: 10.1364/AO.33.002307
- [18] PRAJZLER, V., MAŠTERA, R. Wavelength division multiplexing module with large core optical polymer planar splitter and multilayered dielectric filters. *Optical and Quantum Electronics*, 2017, vol. 49, no. 4, p. 1–11. DOI: 10.1007/s11082-017-0960-4
- [19] PRAJZLER, V., KNIETEL, M., MAŠTERA, R. Large core optical planar splitter for visible and infrared region. *Optical and Quantum Electronics*, 2016, vol. 48, no. 2, p. 1–9. DOI: 10.1007/s11082-016-0444-y
- [20] SENIOR, J. M. *Optical Fiber Communications: Principles and Practice*. 3rd ed., Prentice-Hall, 2008. ISBN: 978-0130326812
- [21] PRAJZLER, V., NEKVINDOVÁ, P., HYPŠ, P. Properties of the optical planar polymer waveguides deposited on printed circuit boards. *Radioengineering*, 2015, vol. 24, no. 2, p. 442–448. DOI: 10.13164/re.2015.0442
- [22] PRAJZLER, V., NEKVINDOVÁ, P., HYPŠ, P., et al. Flexible polymer planar optical waveguides. *Radioengineering*, 2014, vol. 23, no. 3, p. 776–782. ISSN: 1210-2512

- [23] PRAJZLER, V., MAŠTERA, R., JEŘÁBEK, V. Large core planar 1 x 2 optical power splitter with acrylate and epoxy resin waveguides on polydimethylsiloxane substrate. *Radioengineering*, 2014, vol. 23, no. 1, p. 488–495. ISSN: 1210-2512
- [24] PRAJZLER, V., NERUDA, M., ŠPIRKOVÁ, J. Planar large core polymer optical 1x2 and 1x4 splitters connectable to plastic optical fiber. *Radioengineering*, 2013, vol. 22, no. 3, p. 751–757. ISSN: 1210-2512

About the Authors ...

Václav PRAJZLER was born in 1976 in Prague, Czech Republic. He received the MSc and Ph.D. degrees in the Faculty of Electrical Engineering, Czech Technical University in Prague, Czech Republic, in 2001 and 2007, respectively. Since 2014, he has been working as an Associate Professor in the Dept. of the Microelectronics, Faculty of Electrical Engineering, Czech Technical University in Prague. Since 2015, he is a senior member of the IEEE and

his current research is focused on design, fabrication and investigation of properties of polymer photonics structures.

Marian KNIETEL was born 1993 in Považská Bystrica, Slovakia. He received his MSc degree from the Dept. of Microelectronics, Faculty of Electrical Engineering, Czech Technical University in Prague in 2017 and his thesis deals with design, construction and measurement of properties of planar multimode power splitters.

Petr JAŠEK was born in 1993. He received his MSc degree from the Dept. of Microelectronics, Faculty of Electrical Engineering, Czech Technical University in Prague in 2017 and his thesis deals with design, deposition tests and diagnostics of optical multi-mode and single-mode structures fabricated from epoxy and cyclic olefin copolymer materials. He is currently working toward the Ph.D. degree in the Dept. of Microelectronics, Faculty of Electrical Engineering, Czech Technical University in Prague and his current research is focused on design of photonics structures.